Novel, Monomeric Cyanine Dyes as Reporters for DNA Helicase Activity

ARTICLE *in* JOURNAL OF FLUORESCENCE · DECEMBER 2007

Impact Factor: 1.93 · DOI: 10.1007/s10895-007-0215-z · Source: PubMed

J Fluoresc (2007) 17:671–685
DOI 10.1007/s10895-007-0215-z

ORIGINAL PAPER

Novel, Monomeric Cyanine Dyes as Reporters for DNA Helicase Activity

Cuiling Xu · Mykhaylo Yu Losytskyy · Vladyslava B. Kovalska · Dmytro V. Kryvorotenko · Sergiy M. Yarmoluk · Sarah McClelland · Piero R. Bianco

Received: 23 April 2007 / Accepted: 30 May 2007 / Published online: 3 August 2007

Abstract The dimeric cyanine dyes, YOYO-1 and TOTO-1, are widely used as DNA probes because of their excellent fluorescent properties. They have a higher fluorescence quantum yield than ethidium homodimer, DAPI and Hoechst dyes and bind to double-stranded DNA with high affinity. However, these dyes are limited by heterogeneous staining at high dye loading, photocleavage of DNA under extended illumination, nicking of DNA, and inhibition of the activity of DNA binding enzymes. To overcome these limitations, seven novel cyanine dyes (Cyan-2, DC-21, DM, DM-1, DMB-2OH, SH-0367, SH1015-OH) were synthesized and tested for fluorescence emission, resistance to displacement by Mg^{2+}, and the ability to function as reporters for DNA unwinding. Results show that Cyan-2, DM-1, SH-0367 and SH1015-OH formed highly fluorescent complexes with dsDNA. Of these, only Cyan-2 and DM-1 exhibited a large fluorescence enhancement in buffers, and were resistant to displacement by Mg^{2+}. The potential of these two dyes to function as reporter molecules was evaluated using continuous fluorescence, DNA helicase assays. The rate of DNA unwinding was not significantly affected by either of these two dyes. Therefore, Cyan-2 and DM-1 form the basis for the synthesis of novel cyanine dyes with the potential to overcome the limitations of YOYO-1 and TOTO-1.

Keywords Cyanine dye · YOYO-1 · Dye-displacement · DNA helicase assay · RecBCD

Abbreviations

EthD	ethidium homodimer
DAPI	4′,6-diamidino-2-phenylindole
YO-PRO-1	4-[(3-methyl-2(3*H*)-benzoxazolylidene)methyl]-1-[3-(trimethylammonio)propyl]-, diiodide
YO	oxazole yellow
TO	thiazole orange
YOYO-1	1,1′-(4,4,7,7-tetramethyl-4,7-diazaundecamethylene)-*bis*-4-[3-methyl-2,3-dihydro-(benzo-1,3-oxazole)-2-methylidene]-quinolinium tetraiodide
TOTO-1	1,1′-(4,4,7,7-tetramethyl-4,7-diazaundecamethylene)-*bis*-4-[3-methyl-2,3-dihydro-(benzo-1,3- thiazole)-2-methylidene]-quinolinium tetraiodide

Introduction

Real-time, single molecule studies of enzymatic reactions on DNA are significantly enhancing our understanding of

C. Xu · P. R. Bianco
Department of Microbiology and Immunology,
University at Buffalo,
Buffalo, NY 14214, USA

C. Xu · P. R. Bianco
Department of Biochemistry, University at Buffalo,
Buffalo, NY 14214, USA

C. Xu · P. R. Bianco (✉)
Center for Single Molecule Biophysics, University at Buffalo,
Buffalo, NY 14214, USA
e-mail: pbianco@buffalo.edu

M. Y. Losytskyy · V. B. Kovalska · D. V. Kryvorotenko · S. M. Yarmoluk
Institute of Molecular Biology and Genetics,
National Academy of Sciences of Ukraine,
150 Zabolotnogo Street,
03143 Kyiv, Ukraine

Present address:
S. McClelland
Marie Curie Research Institute, The Chart, Oxted,
Surrey, RH8 0TL, UK

DNA–protein interactions [1]. To overcome the size limitation of DNA in single molecule imaging which precludes easy visualization using light microscopy, fluorescent dyes were developed that bind to double-stranded DNA (dsDNA) with high affinity [2]. Morikawa and Yanagida first successfully observed single DNA molecules labeled with the fluorescent dye DAPI in 1981 [2, 3]. This approach has been subsequently used to study DNA condensation [4–6], chromatin assembly [7], DNA digestion by endo- and exonucleases [8, 9], DNA–RecA interactions [10, 11], polymer dynamics [12, 13] and DNA unwinding by helicases, such as the RecBCD enzyme of *Escherichia coli* [14–16].

There are a large number of DNA binding dyes currently available. Some recognize either the major or minor grooves of DNA (i.e., DAPI and the Hoechst dyes), while others intercalate between base pairs of DNA (i.e., ethidium bromide and propidium iodide) [17]. Although these dyes have found widespread use, they have high background in the absence of DNA and bind with relatively low affinity. A more recent addition to the DNA-binding dyes are the cyanine dyes. These are a valuable family of fluorophores, typically have a high quantum yield, large extinction coefficients and moderate photostabilities [18–20]. Cyanine dyes can be readily synthesized by linking the appropriate quaternized, heteroaromatic nuclei through a polymethine bridge [18, 19] or incorporating the affinity modifying groups into the cyanine structure [21]. The cyanine dyes have been widely applied in biology and medicine as fluorescence probes for the detection of DNA and RNA (11), interaction of proteins with DNA [22], protein folding [23] and the activities of DNA polymerases [24]. They are virtually non-fluorescent when free in solution and exhibit a dramatic fluorescent intensity enhancement upon binding to DNA (>1,000-fold for YOYO-1 [25]).

Currently the most widely used cyanine dyes are YO, TO and their homodimers, YOYO-1 and TOTO-1. Dimeric forms of YO and TO were first synthesized by Rye et al. [26]. The dimeric forms consist of two intercalating groups spaced by a linker containing two positive charges (the whole dimmer dye containing thus four charges), giving the dimeric forms a 100-fold higher affinity for nucleic acid than that of the monomeric forms [17]. They bind to DNA with high affinity (K_b in the range 10^{10}–10^{12} M^{-1}), forming complexes with DNA that remain stable even during electrophoresis [25]. Their interaction with DNA is not simple as they have been found to exhibit either a bis-intercalation mode at low dye to base pair ratios, or a less well characterized mode of external binding at high dye to base pair ratios [17]. Unlike to DAPI and Hoechst 33258, these dyes bind to dsDNA in a manner that is generally independent of the DNA base pair composition [26].

Although YOYO-1 and TOTO-1 are excellent dyes, they are not without drawbacks. First, the fluorescent intensity enhancement is sensitive to buffer type and pH, and is affected by mono- and divalent metal ions with a significant reduction observed at concentrations required for many DNA-binding enzymes [27]. The second drawback of YOYO-1 is its tendency to photocleave the probed dsDNA under extended illumination conditions [28]. Third, possibly most significantly, is that YOYO-1 shows notable inhibition of enzyme activity as reported for exo- and endonucleases [8, 9], and DNA helicases [14, 15, 29]. Typically, this inhibition occurs at DNA to dye ratios considerably higher than those observed for dyes such as DAPI and the Hoechst dyes. Collectively, these problems can limit the utility of these dyes as reporter molecules in DNA-binding experiments. Consequently, this has triggered the design of a new generation of cyanine-based dyes, with the intention of overcoming the above-mentioned limits.

In this paper, the synthesis of seven novel monomeric cyanine dyes is described. The structures are presented in Table 1. The effect of buffer type and the concentration of magnesium ions on the fluorescent intensity of each dye–dsDNA complex was examined. The utility of these dyes to function as reporter molecules was determined in a continuous, fluorescent dye based, DNA helicase assay. Results show that the novel fluorescent dyes, Cyan-2 and DM-1, exhibit sharp fluorescent intensity enhancement on DNA binding, have relatively high resistance to displacement by magnesium ions and are effective reporters for DNA unwinding by RecBCD enzyme, the model DNA helicase used in this work. In addition, those dyes bind to dsDNA with affinities similar to YO-PRO-1. More importantly, they bind to ssDNA very poorly, whereas YO-PRO-1 binds to ssDNA with high affinity. As such, they form the basis for the synthesis of a novel class of cyanine dyes with the potential to overcome the limitations of YOYO-1 and TOTO-1.

Materials and methods

Chemicals

All chemicals were reagent grade and were made up in nanopure water and passed through 0.2 μm filters. ATP was purchased from Pharmacia. 2-[(2-Amino-2-oxoethyl)amino]ethanesulphonic acid (ACES), dithiothreitol (DTT), and spectrophotometric grade dimethyl sulfoxide (DMSO) were from ACROS. Trizma base was from SIGMA and 3-[*tris* (hydroxymethyl) methyl] amino propanesulphonic acid (TAPS) was from AVOCADO Research Chemicals Ltd.

DNA

Monomeric, covalently closed circular DNA (pPB67) was purified from *Escherichia coli* strain KK2186 (*SupEΔ (lac-*

proAB) hsdR4 ΔrecA 1398srl::Tn10(tet)) by alkaline lysis [30], which included a LiCl-precipitation step to remove RNA [31]. This was followed by isopycnic centrifugation in cesium chloride gradients [32]. Purified DNA was stored in TE buffer (10 mM Tris–HCl, pH 7.5, 1 mM EDTA) at −20 °C. The nucleotide concentration of dsDNA was determined by measuring the absorbance at 260 nm using the extinction coefficient, ε=6,500 M^{-1} cm^{-1}. M13 ssDNA was prepared as described [33] and the concentration was determined spectrophotometrically using the extinction coefficient, ε=8,784 M^{-1} cm^{-1}. All DNA concentrations are reported in μM nucleotides.

To prepare linear dsDNA, covalently closed circular DNA (pPB67) was linearized using the restriction enzyme *HindIII* (New England Biolabs) in its corresponding buffer for 2 h at 37 °C. Analysis by agarose gel electrophoresis showed complete linearization of the plasmid pPB67. Then the sample was incubated at 70 °C for 15 min to inactivate the restriction enzyme and purified by passing through S-400 microspin columns (Amersham Biosciences) pre-equilibrated with TE buffer. The DNA concentration was subsequently determined using ε=6,500 M^{-1} cm^{-1}.

Proteins

Purification of SSB protein The *Escherichia coli* single-stranded DNA binding protein (SSB) was purified from strain K12ΔH1Δtrp, as described in [34]. The concentration of SSB was determined at 280 nm using ε= 30,000 M^{-1} cm^{-1}. The binding site size of SSB was determined to be 10 nucleotides per monomer by monitoring the quenching of the intrinsic fluorescence of SSB upon binding to ssDNA, as described in [35].

Purification of biotinylated RecBCD enzyme Growth of cells, induction of expression of genes and protein purification details are as provided previously [36]. RecBCD protein was quantitated using an extinction coefficient of ε=40,000 M^{-1} cm^{-1} at 280 nm. The preparation of RecBCD enzyme used in these experiments was 80% active, as determined using a spectrofluorometric helicase assay [37]. For all reactions, the active concentration of RecBCD is given.

Cyanine dyes

The commercially available dyes YO-PRO-1 and YOYO-1 were purchased as DMSO solutions from Molecular Probes (Invitrogen).

Synthesis of novel dyes

We are thankful to Dr. A. Bogolyubskyi (ENAMINE, Kyiv, Ukraine) for providing the dye SH-0367 and to Dr. Yu. Slominskii (Institute of Organic Chemistry, Kyiv, Ukraine) for providing dyes Cyan-2 and SH1015-OH. Trimethine cyanine dye DC-21 was synthesized as described in [38]. Monomethine dyes DM, DM-1 and DMB-2OH were synthesized by the reaction of 2-methylthiobenzothiazolium methosulfate with quaternized heterocyclic salts, having an active methyl group in the presence of triethylamine [39]. Structures of obtained compounds were confirmed with ^{1}H NMR and elemental analysis. The synthesis of dye DM-1 is presented in Scheme 1. For the dyes DM and DMB-2OH, a similar synthetic scheme was applied.

The quaternary salts of 3,4-lutidine, lepidine and 2-methylbenzothiazole were prepared as follows. A mixture of 0.01 mol heterocycle and 0.01 mol 3-chloro-1,2-propanediol was heated for 6 h at 120 °C. Quaternary salts were used without further purification.

For the preparation of dyes, a mixture of 0.001 mol of quaternary salt, 0.001 mol 2-methylthiobenzothiazolium methosulfate, 0.001 mol triethylamine in 4 ml of dry methanol was refluxed for 30 min. Aqueous solution of $NaClO_4$ or KI was added. Crystalline dye precipitate was filtered off and crystallized from methanol.

The structure of the synthesized monomethine dyes was confirmed with ^{1}H NMR spectra and elemental analysis. Data of ^{1}H NMR and CHN analysis for the synthesized dyes are presented below:

DM:

1-(2,3-Dihydroxypropyl)-3-methyl-4-[[3-methyl-2(3*H*)-benzothiazolylidene]methyl]-pyridinium perchlorate, yield: 30%; m.p.:179–182 °C; ^{1}H NMR (DMSO-d_6) δ (ppm):2.34 (3H, s) 3.34(1H, m) 3.47(1H, m) 3.78(3H, s) 3.83(1H, m) 4.09(1H, m) 4.38(1H, m) 4.99(1H, t, *J*=5.4 Hz) 5.34(1H, d, *J*=5.3 Hz) 5.82(1H, s) 7.31(1H, dd, *J*=7.7 Hz) 7.51(2H, m) 7.64(1H, d, *J*=8.2 Hz) 7.93(1H, d, *J*=7.8 Hz) 8.22(1H, s) 8.32(1H, d, *J*=7.2 Hz); Anal.calcd. for $C_{18}H_{25}ClN_2O_6S$: C, 4.94; H, 5.82; N, 6.47. Found: C, 50.12; H, 5.95; N, 6.28.

DM-1:

1-(2,3-Dihydroxypropyl)-4-[[3-methyl-2(3*H*)-benzothiazolylidene]methyl]-quinolinium perchlorate, yield: 62%; m.p.: <250 °C; ^{1}H NMR (DMSO-d_6) δ (ppm): 3.48(1H, m) 3.58 (1H, m) 3.90(1H, m) 4.02(3H, s) 4.26(1H, m) 4.92(1H, m) 5.07(1H, t, *J*=5.4 Hz) 5.32(1H, d, *J*=5.3 Hz) 6.93(1H, s) 7.41 (2H, m) 7.62(1H, dd, *J*=8.1 Hz) 7.77(2H, m) 8.06(3H, m) 8.50(1H, d, *J*=8.3 Hz) 8.81(1H, d, *J*=8.3 Hz); Anal.calcd. for $C_{21}H_{25}ClN_2O_6S$: C, 53.79; H, 5.37; N, 5.97. Found: C, 53.98; H, 5.10; N, 6.12.

DMB-2OH:

3-(2,3-Dihydroxypropyl)-2-[[3-methyl-2(3*H*)-benzothiazolylidene]methyl]-benzothiazol-3-ium iodide, yield: 67%; m.p.:<250 °C; ^{1}H NMR (DMSO-d_6) δ (ppm): 3.57(2H, m) 3.97(3H, s) 4.02(1H, m) 4.62(2H, m) 5.25(1H, t, *J*=5.5 Hz) 5.36(1H, d, *J*=5.4 Hz) 6.87(1H, s) 7.50(2H, m) 7.68(2H, m)

Scheme 1 Synthesis of the dye DM-1

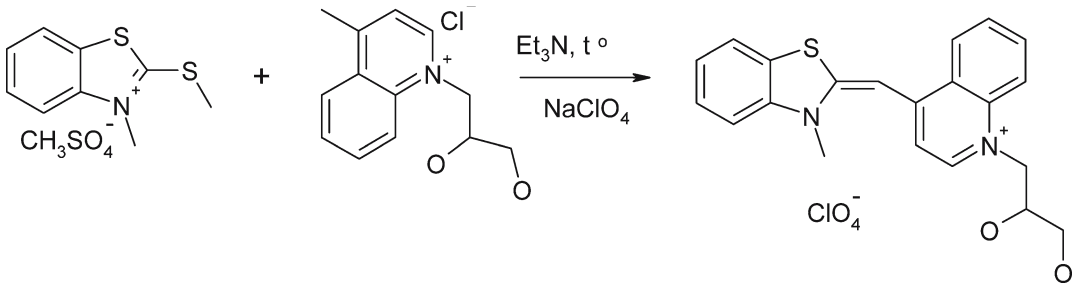

7.87(2H, m) 8.22(2H, d, J=8.1 Hz); Anal.calcd. for $C_{19}H_{21}IN_2O_2S_2$: C, 45.60; H, 4.23; N, 5.60. Found: C, 45.21; H, 4.11; N, 5.84.

Preparation of dye stock solutions

The seven novel dyes were dissolved in spectrophotometric grade DMSO as stock solutions and then stored as aliquots at −80 °C. The concentration of each dye was determined on each day of use by measuring the absorbance in a Cary Eclipse spectrophotometer and using the extinction coefficients given in Table 1.

Fluorescence experiments

Fluorescence measurements were carried out in a Cary Eclipse fluorescence spectrophotometer (Varian, Australia) with continuous stirring provided by magnetic stir bars inside 0.5 cm quartz cuvettes. The reaction temperature of 20 °C was maintained by a PCB150 peltier-controlled water circulator to an accuracy of ±0.5 °C.

DNA and Mg^{2+} titrations Starting reactions (500 μl) contained 0.1 or 1 μM dye in either dH_2O (pH 6.8), or 30 mM buffer: ACES (pH 7.3), TrisOAc (pH 7.5), TAPS (pH 8.5). Once the dye solution was monitored, small volumes of linear dsDNA were added in 1 μM increments to the dye solutions. Once the fluorescent signal had stabilized, the next aliquot of DNA was added. This was repeated until addition of DNA produced no further change in the fluorescence signal. The time to reach signal stabilization varied with dye and buffer condition, ranging between 10–100 s (data not shown). Once the final DNA concentration had been reached, 1 or 5 μl of 1 M $Mg(OAc)_2$ was added, resulting in a 2 or 10 mM increment, respectively. Similarly, $Mg(OAc)_2$ aliquots were not added to the reaction unless the fluorescent signal had stabilized between the intervals of addition.

Data from the DNA titrations were analyzed to determine binding constants. First, using nonlinear regression, the fluorescence data were fit to a hyperbola ($F = F_{max}[DNA]/([DNA] + K_d)$), F: the stable fluorescence intensity of each DNA aliquot addition; F_{max}: the max fluorescence intensity at saturated DNA concentration; [DNA]: the final DNA concentration after each DNA aliquot addition; K_d: the binding constant of dye to DNA) to estimate the binding constant, K_d. Further analysis of data was done using Scatchard plots, which were linear for dsDNA and non-linear for ssDNA (data not shown).

Helicase assays These were performed in a 500 μl reaction mixture consisting of Mix I (20 mM TrisOAc pH 7.5, 1 mM DTT, 2 mM $Mg(OAc)_2$, 1 μM SSB, 0.25 nM active RecBCD enzyme), Mix II (10 μM dsDNA alone or 10 μM dsDNA bound to 0.5 μM dye) and 1 mM ATP. The appropriate amount of DNA and dye were mixed and incubated at 20 °C for 20 min before adding to Mix I. Reactions were initiated by the addition of ATP to 1 mM final concentration, following a 5-min pre-incubation of all other components at 20 °C. The excitation and emission wavelengths were set at 290 and 340 nm, respectively, to measure the intrinsic fluorescence of SSB protein. The decrease in fluorescent intensity of the cyanine dyes was followed using the appropriate excitation and emission wavelengths (see Table 1). The slit widths were 2.5 and 5 nm for excitation and emission slits, respectively, in both SSB protein and dye fluorescence experiments. When both SSB and dyes were present in the reaction mixture, a multi-wavelength, temperature controlled kinetics program was used (Cary Eclipse software). Therefore, we were able to simultaneously monitor the intrinsic fluorescence of SSB and fluorescent dye intensity. The excitation and emission wavelengths for SSB and dyes are far enough apart to avoid inner filter effects.

Results

Cyanine dyes exhibit significant fluorescence enhancement upon binding to dsDNA

For single molecule detection techniques or other techniques requiring sensitive detection of dsDNA, dyes must

Table 1 Parameters of cyanine dyes used in this work

Dye name	Dye structure	$\varepsilon_{DMF}\times10^5$ $M^{-1}cm^{-1}$ [a]	$\lambda_{ex}/\lambda_{em}$ /nm
Cyan-2	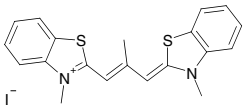	0.83	545/563
DC-21	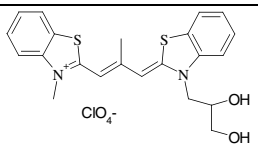	0.82	551/567
DM	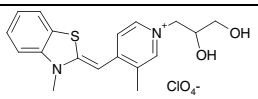	0.53	462/478
DM-1	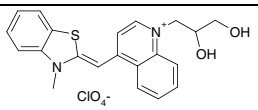	0.63	513/530
DMB-2OH	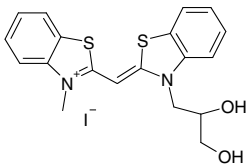	0.71	434/462
SH-0367	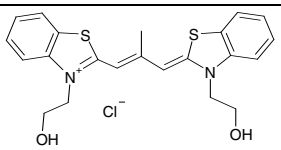	1.04	557/568
SH1015-OH	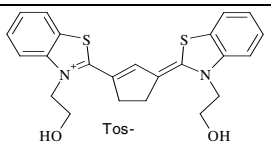	1.4	616/628
YO-PRO-1[b]	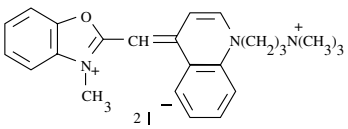	0.52	491/509

[a] Molar extinction coefficient of dye in dimethylformamide (DMF) solution

[b] YO-PRO-1 was supplied in dimethylsulfoxide (DMSO).

exhibit a significant enhancement of fluorescent intensity upon binding to dsDNA relative to the free dye, or to the dye bound to ssDNA. To determine whether each of the novel monomeric cyanine dyes exhibited fluorescent intensity enhancement on DNA binding, aliquots of dsDNA were added to a fixed concentration of dye and the resulting change in fluorescence was recorded.

First, to eliminate potential complications due to buffer type or pH, experiments were conducted in water (pH 6.8) only. Rye et al. reported that reproducible and stable complexes of cyanine dyes with dsDNA could be formed when dsDNA was added to the dye solution, but not if the mixing order was reversed [26]. Thus, in separate reactions, DNA was added in small increments to a constantly stirred solution of each dye. Once the fluorescence signal had stabilized (typically 10–100 seconds), the fluorescence spectrum was recorded and a second aliquot of DNA was added. This process was repeated until no additional enhancement in signal was obtained. These data are presented in Fig. 1.

The results in water only (Fig. 1a) show that all dyes except SH1015-OH, exhibited negligible fluorescence in the absence of DNA and significant fluorescent intensity enhancement on DNA binding. Cyan-2, DC-21, DM-1 and SH-0367 have typical saturation curves in this dsDNA range, whereas DM and DMB-2OH do not, which may result from very low affinity to dsDNA even at ratios of 20 bp per dye molecule. The fluorescence intensity en-

hancement in water ranged from a low of 5 for SH1015-OH to a maximum of 459 observed for DC-21 (Table 2).

Although the structure of a dye is a critical issue for the fluorescence enhancement that occurs on DNA binding (Fig. 1a), buffer type and/or pH may affect the extent of fluorescent intensity enhancement as well. To further examine the influence of buffer type or pH on the fluorescence enhancement of dye–dsDNA complexes, DNA titrations were performed in ACES (pH 7.3), TrisOAc (pH 7.5), and TAPS (pH 8.5) buffers. TrisOAc is used as it is perhaps one of the more widely used buffers in biological research. TAPS and ACES are used as these buffers provide excellent signal/noise in single molecule experiments using YOYO-1 (data not shown). The resulting, typical titration curves are shown in Fig. 1b–d.

All of the dyes tested display typical saturation curves in buffers, and further, the fluorescent intensity of each dye is greater than that observed in water with the exception being DC-21. Surprisingly, the fluorescence enhancement of DC-21 decreased 4.5-fold in the presence of buffers relative to that observed in water (Table 2). For the majority of the dyes, the fluorescence enhancement was the highest in TrisOAc buffer (Fig. 1c, Table 2). For both Cyan-2 and DM-1, the enhancement in TrisOAc was only slightly lower than that observed in ACES or TAPS buffer. For SH1015-OH, a strong fluorescence signal was observed in the presence of DNA that is the highest of all the novel dyes (Fig. 1). However, due to the high signal in the absence of the DNA, the fluorescence intensity enhancement is only 7±1, independent of solution conditions (Table 2). For the remaining five dyes, the fluorescence enhancement was generally higher in buffers than in water, with Cyan-2 and DM-1 producing the highest enhancement of 423±72 and 631±12, respectively (Table 2). For DM-1, the fluorescence intensity enhancement was independent of buffer type and pH while for Cyan-2, enhancement increased as buffer pH decreased from 8.5 to 7.3 (Table 2). Although both Cyan-2 and DM-1 exhibit a large fluorescent intensity enhancement on DNA binding, this enhancement is significantly lower than that observed for YO-PRO-1.

To evaluate the affinity of each dye for DNA, data from the DNA titrations shown in Fig. 1 were analyzed using Scatchard plots. The Scatchard plot for each dye was linear, indicating non-cooperative binding (data not shown), and the resulting, calculated binding constants are shown in Table 3. The data show that the highest affinity for dsDNA was obtained for Cyan-2, DM and SH1015-OH (Table 3). These K_d values are 1.9-fold lower than that obtained for YO-PRO-1. Intermediate affinities were observed for DC-21 and DMB-2OH while those for DM-1 and SH-0367 were comparable to that of YO-PRO-1. As for the fluorescence intensity enhancement (Table 2), K_d is also influenced by buffer type and pH. However, the effects on K_d are different from those on fluorescence enhancement. For example, the K_d for Cyan-2 binding to dsDNA is independent of solution conditions, while for DM and SH1015-OH, K_d increases 127- and 33-fold respectively in the absence of buffer (Table 3). However, it should be noted that for DM, DMB-2OH and SH1015-OH, the K_d values are at best, approximations since saturation of fluorescence signal could not be achieved (data not shown).

In addition to measuring affinity for dsDNA, the affinity of four dyes for M13 ssDNA was also determined. Titrations of ssDNA relative to dyes were done in identical fashion to those shown in Fig. 1 and values for K_d were obtained from Scatchard plots. In contrast to the data for

Table 2 The novel cyanine dyes, Cyan-2 and DM-1, exhibit the largest buffer-independent enhancement on binding to dsDNA

Dye	Fluorescent Intensity Enhancement (F_{bound}/F_{free})[a]				
	H_2O (pH 6.8)	ACES (pH 7.3)	TrisOAc (pH 7.5)	TAPS (pH 8.5)	Buffer average*
Cyan-2	326	501	408	360	423±72
DC-21	459	73	164	73	103±53
DM	99	148	163	138	150±13
DM-1	95	633	618	642	631±12
DMB-2OH	97	111	127	117	118±8
SH-0367	173	157	214	59	143±78
SH1015-OH	5	7	8	6	7±1
YO-PRO-1	723	785	794	786	788±5

[a] This ratio was calculated using the maximum fluorescence signal obtained at saturating concentration of DNA (20 μM) and divided by the fluorescence signal in the absence of DNA. For several dyes, no signal was detected in the absence of DNA. Therefore, a value of 1 was used instead. Novel dyes were measured at high PMT detector voltage, slit width: 2.5/5 nm. YO-PRO-1 was measured at medium PMT detector voltage.

*The values were obtained by averaging the enhancement of each dye in each buffer.

Table 3 Binding constants for single and double-stranded DNA

Dye	K_d (μM^{-1})					
	dsDNA*					ssDNA**
	H_2O (pH 6.8)	ACES (pH 7.3)	TrisOAc (pH 7.5)	TAPS (pH 8.5)	Buffer average	TrisOAc (pH 7.5)
Cyan-2	1.5±0.2	1.6±0.1	2.1±0.3	1.6±0.2	1.8±0.3	35.1±4.4
DC-21	2.9±0.4	1.9±10.3	6.2±1.6	2.6±0.2	3.6±2.3	ND
DM	292.3±353	2.6±0.2	1.2±0.2	3.2±0.2	2.3±1.0	ND
DM-1	4.5±0.4	9.9±2.4	10.9±0.9	5.3±1.2	8.7±3.0	8.9±0.6
DMB-2OH	194±200	5.6±1.2	3.5±0.2	2.1±0.2	3.7±1.8	ND
SH-0367	5.5±0.4	4.6±0.3	7.5±0.4	5.8±0.3	6.0±1.5	ND
SH1015-OH	52.1±10.1	1.8±0.6	2.3±0.5	0.8±0.4	1.6±0.8	26.0±4.8
YO-PRO-1	4.4±0.5	6.0±0.9	7.5±0.8	6.9±0.7	6.8±0.8	11.9±0.7

Data were obtained from DNA titration to a fixed concentration of 1 μM dye solution in various solutions except ssDNA titration only in TrisOAc buffer at 20 °C (same condition as Fig. 1). All titrations were performed once. Novel dyes were measured at high PMT detector voltage, slit width: 2.5/5 nm. YO-PRO-1 was measured at medium PMT detector voltage for dsDNA titration and high PMT detector voltage for ssDNA titration, respectively.

*Units are in base pairs.

**Units are in nucleotides.

dsDNA, the Scatchard plots were non-linear, indicating cooperative binding of dyes to ssDNA. Therefore, the K_d values are only approximations. Surprisingly, Cyan-2 and SH1015-OH exhibited a greater than 10-fold lower affinity for ssDNA, while DM-1 and YO-PRO-1 displayed comparable affinities for either DNA type (Table 3). Furthermore, Cyan-2 has over a three-fold higher binding affinity than YO-PRO-1 for either DNA type.

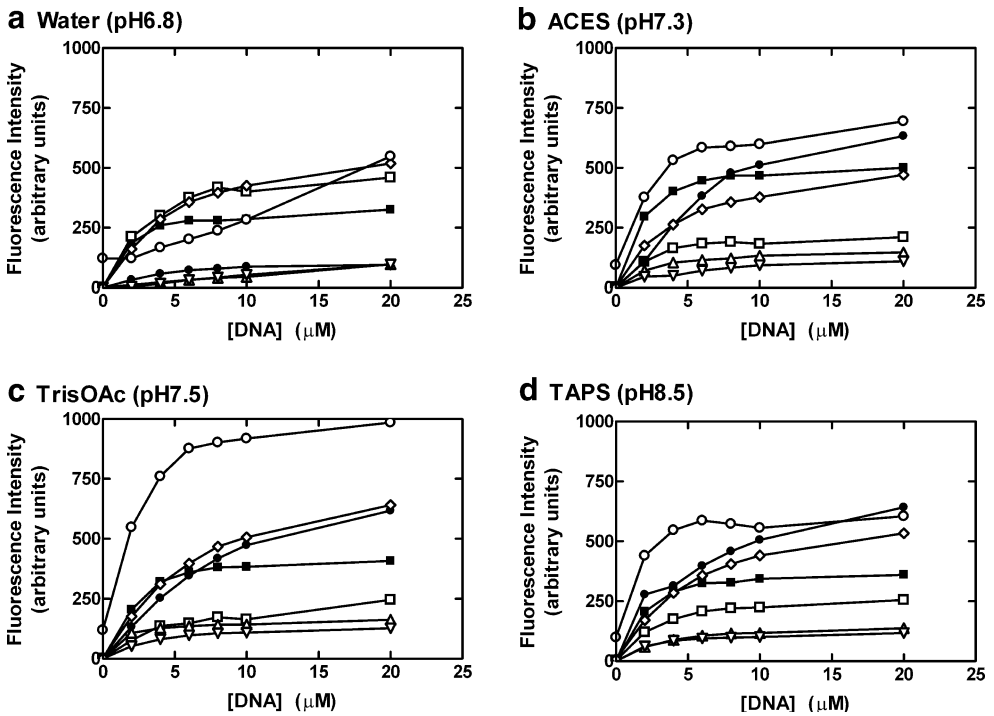

Fig. 1 Fluorescence enhancement on binding to dsDNA is affected by dye structure and solution conditions. Experiments were performed by the addition of aliquots of dsDNA to a fixed concentration of 1 μM dye solution in each buffer at 20 °C. The fluorescent intensity was measured using the excitation/emission wavelength for each dye listed in Table 1 and em/ex slit widths of 2.5 and 5 nm. The values reported at each concentration of DNA are from the resulting stable fluorescence signals following each addition. Increase in fluorescent intensities of Cyan-2 (*filled squares*), DC-21 (*empty squares*), DM (*triangles*), DM-1 (*filled circles*), DMB-2OH (*inverted triangles*), SH-0367 (*diamonds*) and SH1015-OH (*empty circles*) upon addition of linear dsDNA in the presence of water (pH 6.8) (**a**), ACES (pH 7.3) (**b**), TrisOAc (pH 7.5) (**c**) and TAPS (pH 8.5) buffer (**d**)

Cyan-2 and DM-1 exhibit the highest resistance to displacement by magnesium ions

Liu et al. [40] reported that divalent metal ions, such as magnesium ions, quench the fluorescence signal of the YOYO-1-DNA complex by competitive binding to DNA. If the dyes presented here are to be used in subsequent studies to replace YOYO-1, the dye-DNA complexes should be more resistant to the displacement by magnesium ions than the monomeric form of YO or TO. To determine the resistance of Cyan-2 and DM-1 dye–DNA complexes to displacement by magnesium ions, DNA–dye complexes were formed and challenged by the addition of small volumes of 1 M $Mg(OAc)_2$. To determine whether the buffer affects the ability of dye to resist the displacement by Mg^{2+}, experiments were carried out in each of three buffers, and water as before.

As expected, the fluorescence signal of dye–dsDNA complexes was sensitive to Mg^{2+} concentration. Cyan-2 is more resistant to displacement by magnesium ions than DM-1, with a 50% reduction in fluorescence being observed at 8±1 mM whereas it is almost 2-fold lower for DM-1 (5±0.5 mM; Fig. 2 and Table 4). Further, at 50 mM $Mg(OAc)_2$, more than 75% of the starting fluorescent signal of either complex is lost.

To determine whether each of the remaining dyes were resistant to displacement by Mg^{2+}, Mg^{2+} titrations identical to those shown in Fig. 2 were done for each novel dye. The concentration of Mg^{2+} causing 50% reduction in fluorescent intensity was calculated and is shown in Table 4. Cyan-2 exhibits the greatest resistance to displacement, followed by YO-PRO-1 and then DM-1. The DM, DMB-2OH and SH1015-OH dyes are extremely sensitive to displacement by Mg^{2+}, as concentrations of only 2 mM are needed to produce a 50% reduction in fluorescent intensity.

Novel cyanine dyes function as reporter molecules in RecBCD DNA helicase assays

Several assays have been developed to measure the unwinding of dsDNA [15, 37, 41, 42]. Two of these are continuous assays that involve monitoring a change in fluorescence. The first assay [37] takes advantage of the intrinsic fluorescence of the *Escherichia coli* single-stranded DNA binding protein (SSB protein), which is quenched upon binding to ssDNA, the product of the unwinding reaction. Thus, as a DNA helicase proceeds to translocate and unwind dsDNA, SSB protein binds to the nascent ssDNA, resulting in the quenching of the intrinsic fluorescence of SSB. Since many DNA helicases can be inhibited by SSB, a complementary assay was developed by the Kowalczykowski lab [15]. Here fluorescent dyes bind to dsDNA resulting in their fluorescence enhancement. As the DNA helicase translocates and unwinds the DNA duplex, dye molecules are displaced resulting in a decrease in fluorescent intensity. A decrease in the fluorescence signal is proportional to the amount of ssDNA produced by a DNA helicase. Consequently, the unwinding rate and extent of reaction for a DNA helicase can be determined by measuring the decrease in fluorescence signal as the dye is displaced from dsDNA. This assay was successfully demonstrated using both minor groove binding (DAPI, Hoechst 33258) and intercalating dyes (TO, EthD) [15].

Schematics of the assay and typical traces for SSB protein fluorescence and dye-displacement DNA helicase assays are shown in Fig. 3. The assay shown uses the well characterized RecBCD of *E. coli*, an excellent model enzyme to study DNA unwinding. In phase I, the signal from the intrinsic fluorescence of SSB protein or the complexes of dyes with dsDNA is stable. In Phase II, unwinding is initiated by the addition of ATP or RecBCD

Table 4 The Cyan-2–DNA complex exhibits the greatest resistance to displacement by magnesium ions

Dye	Magnesium titration midpoint or MTMP (mM)				
	H_2O (pH 6.8)	ACES (pH 7.3)	TrisOAc (pH 7.5)	TAPS (pH 8.5)	Mean
Cyan-2	**9**	**7**	**7**	**7**	**8**±1
DC-21	4	3	4	4	4±0.5
DM	2	2	2	2	2
DM-1	5	5	5	4	5±0.5
DMB-2OH	2	2	2	2	2
SH-0367	4	4	4	4	4
SH1015-OH	2	2	2	2	2
YO-PRO-1	6	6	**7**	6	7±0.5

All titrations were performed once. The MTMP corresponds to magnesium concentration at which the fluorescence signal is reduced by 50%. Bold values indicate the highest MTMP observed under the conditions tested.

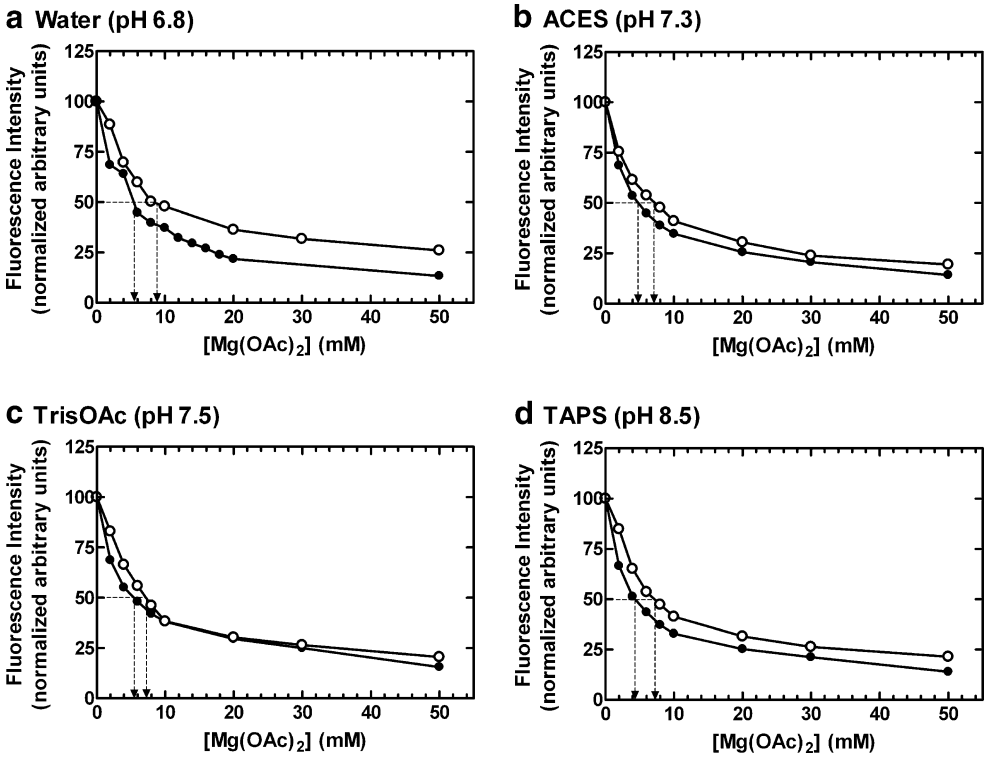

Fig. 2 Cyan-2 and DM-1 are displaced from dsDNA by magnesium ions. Decrease in fluorescent intensity of Cyan-2 (*empty circles*) and DM-1 (*filled circles*) with dsDNA complexes upon addition of Mg^{2+} in the presence of water (pH 6.8) (**a**), ACES (pH 7.3) (**b**), TrisOAc (pH 7.5) (**c**) and TAPS (pH 8.5) buffer (**d**). The arrows in each panel indicate the magnesium titration midpoint in each reaction. Experiments were performed by the addition of aliquots of $Mg(OAc)_2$ to a solution of 10 μM bp dsDNA including 1 μM of either Cyan-2 or DM-1 at 20 °C. The ratio of DNA bp/dye is 10. The fluorescent intensity was measured using the excitation/emission wavelength of 545/563 nm for Cyan-2 and 513/530 nm for DM-1 with em/ex slit widths of 2.5 and 5 nm, respectively. Values for the MTMP for all dyes are shown in Table 4

(indicated by the arrow in Fig. 3b). The fluorescence signal decreases dramatically due to either the dissociation of prebound dyes or the quenching of the intrinsic fluorescence of SSB protein which occurs upon binding to the nascent ssDNA produced by the helicase activity of RecBCD. The fluorescence decrease is easily monitored by a fluorescence spectrophotometer and precisely reflects the helicase activity of RecBCD on dsDNA as demonstrated previously [15, 37]. When unwinding is completed in approximately 60 s (at t=120 s), no change in the now reduced fluorescent signal is observed, indicating that all available dsDNA has been unwound (phase III). The slope of the line ($\Delta f/\Delta t$) fitted to the data points in phase II is used to calculate the initial rate of unwinding, while the difference in total fluorescence (ΔF), represents the extent of unwinding (Fig. 3b). The maximum achievable extent of reaction was established in separate, control reactions by adding an equimolar amount of ssDNA to reaction mixtures containing either SSB alone for SSB binding or dye alone for dye displacement ($\Delta F = F_{\mathrm{dsDNA}} - F_{\mathrm{ssDNA}}$). The initial rate of unwinding was divided by the extent of unwinding and then multiplied by the concentration of base pairs in the reaction to yield the apparent rate in nM bp/s. Thus, if a dye can function as a reporter for DNA unwinding, then a rapid decrease in fluorescence signal is anticipated with a resulting negative ΔF.

To determine whether the novel, monomeric cyanine dyes could function as reporters for DNA unwinding, each dye was tested in the fluorescence-based helicase assay. The concentration of dye used here was 500 nM, a concentration used to eliminate the lag behavior resulting from the redistribution of dye molecules to vacant binding sites on dsDNA [15]. Furthermore, based on our work with YOYO-1 (data not shown) and by comparison to the previous study [15], this concentration of monomeric dye should not inhibit the helicase activity of RecBCD. Further, SSB was included in reactions to bind to nascent ssDNA and monitor DNA unwinding independently and concurrent with dye displacement. Thus, in the data presented herein, a time-dependent decrease in the fluorescence of DNA–dye complexes and the intrinsic fluorescence of SSB protein is simultaneously monitored during the unwinding of dsDNA by RecBCD (examples of typical unwinding traces are shown in Fig. 4a and b). If the dyes used in the reaction do not inhibit the activity of RecBCD on dsDNA, the unwinding rate should be identical to that observed in the absence of dye, i.e., when monitoring SSB fluorescence.

Using the quenching of the intrinsic fluorescence of SSB, the DNA unwinding rates for RecBCD are 28 nM bp/s in the absence of dye, and 27 and 25 nM bp/s in the presence of Cyan-2 and DM-1, respectively (Fig. 4). When monitoring dye-displacement, the unwinding rates are 18 nM bp/s

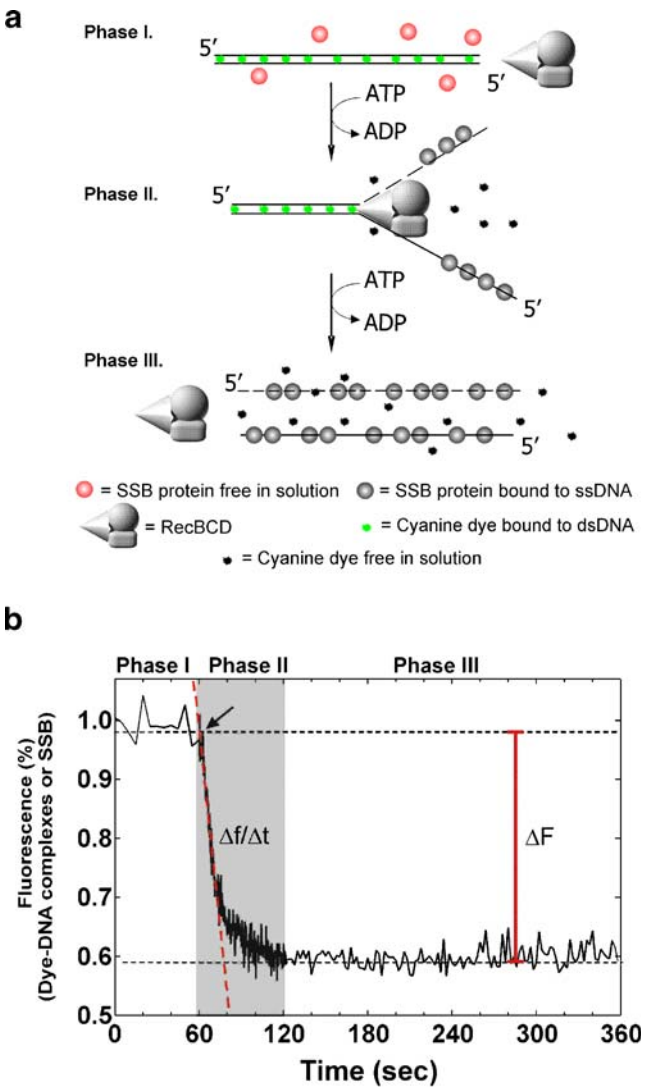

Fig. 3 Schematic of the continuous fluorescence assay used to measure DNA helicase activity. **a** Schematic of the simultaneous SSB protein fluorescence-quenching and dye-displacement assay is shown. **b** Typical time-course curves for both assays. The fluorescence signal at the beginning of the reaction is due to the intrinsic fluorescence of SSB protein in solution (*red circles*) or the fluorescence of the dye–dsDNA (*green stars*) complexes (phase I). As the dsDNA is unwound by RecBCD, SSB protein binds to nascent ssDNA, resulting in the quenching of SSB fluorescence (*black circles*). Concurrently, dye molecules are displaced from dsDNA and rebind to ssDNA or remain free in solution (*black stars*) (phase II). When the unwinding reaction is complete, the fluorescence signal is invariant as a function of time (phase III)

for Cyan-2 and 16 nM bp/s for DM-1, respectively. These values are similar to the value of 20–22 nM bp/s obtained by Eggleston et al. for other monomeric dyes [15]. Thus, Cyan-2 and DM-1 exhibit little or no inhibition of the helicase activity of RecBCD.

To permit direct comparison, the unwinding traces (Fig. 4a and b) were normalized to the starting fluorescence of either SSB or the dye–DNA complexes (Cyan-2 and DM-1), and then expressed as percentage of the starting fluorescence signal (Fig. 4c). When analyzed in this way, the shape of the curve for the SSB protein-fluorescence assay is very similar to that of the dye-displacement assay. However, the ΔF is different for SSB and dyes (Cyan-2 and DM-1), since displacement of dye from dsDNA and rebinding to ssDNA does not lead to the complete quenching of fluorescence intensity. In addition, the presence of SSB in the reaction causes the displacement of a small fraction of dye molecules from ssDNA (data not shown). The Mg-displacement of dye may also contribute to the larger ΔF for Cyan-2 and DM-1 than that for SSB.

For helicase assays, not only is the fluorescent intensity enhancement of dyes bound to dsDNA (relative to ssDNA or free in solution) important, but the fluorescent intensity value is critical for assay sensitivity. As the remaining five dyes did exhibit significant fluorescence increase in the presence of dsDNA, they were tested in the DNA helicase assay. For DC-21, an unwinding rate 24 nM bp/s was observed. Unfortunately, the complex of DC-21 with dsDNA gives a lower fluorescent intensity and less resistance to the displacement by magnesium ions in buffers. For SH-0367, the unwinding rate is reduced 2-fold to 13 nM bp/s, indicating inhibition of the helicase activity of RecBCD. The fluorescence of the dye–DNA complexes of DM, DMB-2OH and SH1015-OH, do not decrease as a function of time over the course of the reaction, even though the DNA is unwound as evidenced by quenching of the intrinsic fluorescence of SSB (data not shown). As they do not follow the SSB protein-fluorescence trace, those dyes are not regarded as suitable reporters for DNA helicase assays.

Novel monomeric cyanine dyes do not inhibit RecBCD whereas YOYO-1 does

YOYO-1 binds to dsDNA with high affinity (K_a =6×10^8 M^{-1}) [43] and has found widespread use in protein–DNA and DNA studies. YOYO-1, however, can inhibit the activity of many proteins including RecBCD (see below). Therefore, to determine whether these monomeric cyanine dyes could inhibit helicase activity, we compared the unwinding rates of RecBCD on the fluorescent dye–DNA complexes of Cyan-2 and DM-1 to those of YO-PRO-1 and YOYO-1.

The reaction conditions were the same as those in Fig. 4 and reactions were initiated by the addition of ATP. The DNA unwinding time courses monitoring quenching of the intrinsic fluorescence of SSB protein in the presence and absence of dyes are shown in Fig. 5a. To permit direct comparison of fluorescence traces, fluorescence signals were normalized to the starting fluorescence signal of

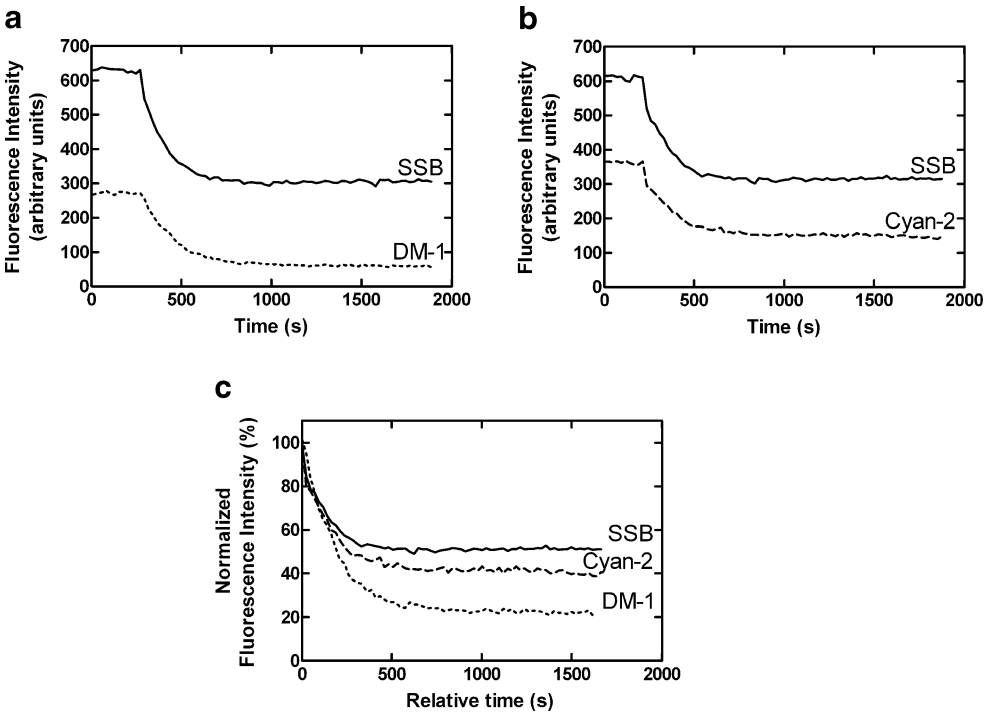

Fig. 4 Cyan-2 and DM-1 function as reporter molecules in RecBCD unwinding assays. DNA unwinding assays were performed with 0.5 μM DM-1 (**a**) or 0.5 μM Cyan-2 (**b**). Reactions contained 0.25 nM RecBCD, 1 μM SSB and 10 μM linear pPB67. **c** Normalized data from panels **a** and **b**. The fluorescence signal was normalized to the signal obtained immediately prior to the addition of ATP to start the reactions. Similarly, reactions times were normalized to the point at which reactions were initiated. The unwinding reactions were performed at 20 °C, and initiated by the addition of ATP, following a 5-min incubation of all the reaction components. The rate of unwinding was followed using the decrease in fluorescent intensity from SSB (ex/em 290/340), DM-1 (ex/em 513/530) or Cyan-2 (ex/em 545/563) using slit widths of 2.5 and 5 nm

SSB prior to initiation of the reaction. The resulting kinetic traces in the presence and absence of dyes are similar but with different unwinding rates and ΔF. In the absence of dye (i.e., SSB only), the reaction yields the largest ΔF, whereas the ΔF is the lowest in the presence of YOYO-1. In the presence of the monomeric dyes Cyan-2, DM-1 and YO-PRO-1, an intermediate ΔF is observed. The unwinding rates calculated from raw data without normalization are displayed in Fig. 5b. The rate of unwinding in the presence of DM-1 (25 nM bp/s), Cyan-2 (27 nM bp/s) and YO-PRO-1 (24±2.1 nM bp/s) is, within experimental error, the same as that observed in the absence of dye (28± 0.9 nM bp/s). In contrast, the rate of unwinding in the presence of YOYO-1, 5±1.0 nM bp/s, is 5.6-fold less than that in presence of either Cyan-2, DM-1 or YO-PRO-1, indicating that at comparable dye concentration, dimeric cyanine dyes inhibits the helicase activity of RecBCD whereas the monomeric dyes do not.

Discussion

The primary conclusion of this work is that two novel cyanine dyes, Cyan-2 and DM-1, bind to dsDNA with relatively high affinity producing a significant fluorescence enhancement. Binding is unaffected by buffer type and pH. Those two dyes also resist displacement by magnesium ions (compared to the remaining five dyes). Further, they do not inhibit the DNA unwinding activity of a model helicase, the *E. coli* RecBCD enzyme. Consequently, they will form the starting point for additional studies to develop novel dimeric cyanine dyes.

To develop novel, specific, fluorescent dyes as reporter molecules for dsDNA and protein–dsDNA interactions in ensemble and single molecule experiments, a new series of cyanine dyes were synthesized (Table 1). They were made by either the incorporation of a hydroxyl group into the cyanine structure, changing the length of the linker, or β-methyl substituted modification [21, 44]. Except for SH1015-OH, these dyes have virtually negligible fluorescence when free in aqueous solution (Fig. 1). The fluorescent intensity of each dye–DNA complex in water is different, which can be ascribed to the different primary structure or modification on the structure. The introduction of a hydroxyl group or lysine template into the structure of the cyanine dyes causes an increase in the emission intensity of dsDNA complexes [44]. For SH-0367 and DC-21, the hydroxylated varieties of Cyan-2, the fluores-

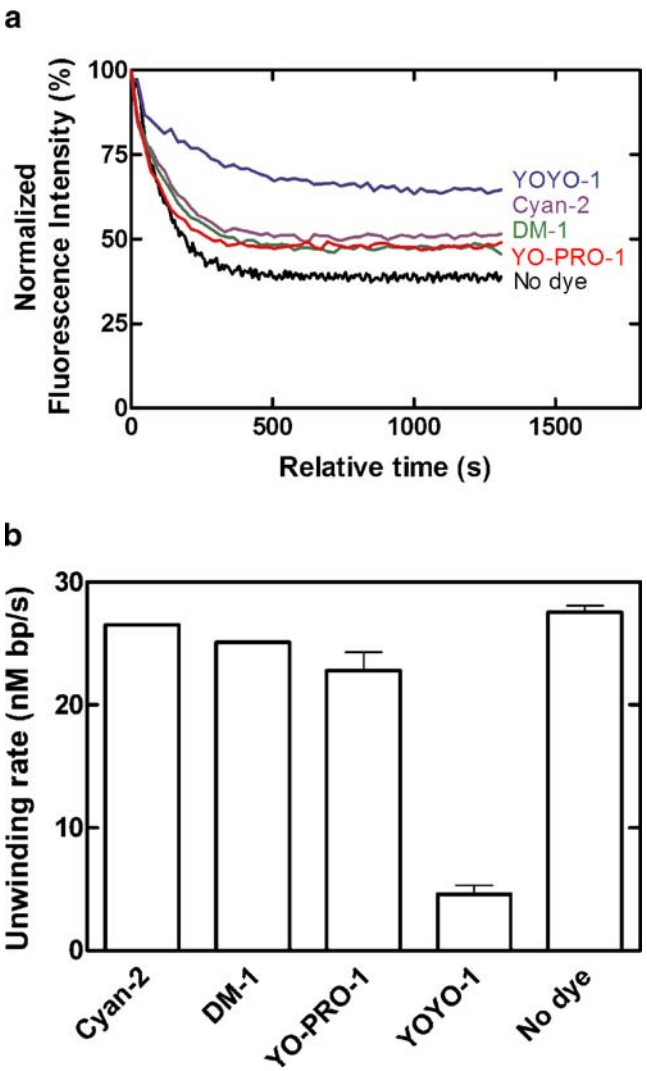

Fig. 5 Monomeric cyanine dyes do not significantly inhibit RecBCD enzyme. **a** Comparison of unwinding rates from reactions done using conditions identical to those in Fig. 4. Data were normalized relative to the starting fluorescence observed immediately prior to reaction initiation. Similarly, time was normalized to the reaction start time for all reactions. Dye was used at 0.5 μM and DNA was at 10 μM. Reactions were performed at 20 °C and initiated by the addition of ATP. The rate of unwinding was followed using the decrease in fluorescent intensity from SSB (ex/em 290/340) with slit widths of 2.5 and 10 nm. **b** Unwinding rates were calculated from time courses shown in panel **a**. Data for Cyan-2 and DM-1 came from a single experiment while those from YO-PRO-1, YO-YO-1 and no dye (SSB only) were done twice

cent intensity in water is higher than the parent dye, possibly due to introduction of the hydroxyl group. The fluorescent intensity of DC-21 was much higher than that of DMB-2OH, due to the longer polymethine chain length of DC-21 reducing the steric hindrance for intercalation into dsDNA. The higher fluorescent intensity of DM-1 than DM is most likely due to the addition of the aromatic ring. The incorporation of cyclopenthene group instead of the β-methyl one into the polymethine chain negatively affects the ability of cyanine dyes to bind to DNA, as evidenced by the comparison of SH-0367 to SH1015-OH (Tables 1 and 2). The presence of positively charged nitrogen, similar to that of the hydroxyl group, can result in the strengthening of dye–dsDNA complexes and an increase in fluorescent intensity, as observed for YO-PRO-1. Therefore, the modification of the cyanine structure in heterocyclic residues and polymethine chain significantly affects the fluorescence enhancement of cyanine dyes that is observed on binding to DNA.

In addition to dye structure, buffer type and pH also influence the fluorescence of the dye–dsDNA complexes. The effects are complicated as some dyes exhibit greater fluorescence enhancement in buffer relative to water while for others, the opposite effect is observed. For example, the fluorescence signal of the DC-21–dsDNA complex is dramatically reduced in buffers relative to that in water (Fig. 1 and Table 2). In contrast, the fluorescent intensity enhancement for DM-1 increases 6.6-fold in buffers relative to that observed in dH_2O (Table 2). The fluorescent intensity enhancement of Cyan-2 and SH-0367, which are similar in structure, is largely unaffected by the presence of buffers relative to dH_2O. For Cyan-2, the fluorescence enhancement is pH-dependent with a lower signal being observed at elevated pH (Table 2), which for SH-0367, this may be a combination of buffer type and pH. The effect of buffer type or pH is not simply due to a change in affinity of the dye for dsDNA (Table 3). The statement holds true for the majority of the dyes examined, although DC-21 and DMB-2OH are notable exceptions (Table 3). Importantly, the enhancement of DM-1 is both buffer- and pH-independent and binding affinity is comparable to YO-PRO-1. The fluorescent intensity of YO-PRO-1 is independent of solution conditions and is more dramatically enhanced in the presence of DNA (788-fold) than that either Cyan-2 (423) or DM-1 (631). This may be mainly due to two positive charges on YO-PRO-1 (Table 1), which increases the fluorescent intensity of the dye–DNA complexes.

The modification of the cyanine dye structure has complex effects on the affinity for DNA that may be further complicated in the presence of buffers (Table 3). The introduction of the substituent containing hydroxyl group into the dye heterocycle increases the fluorescence intensity of dye–DNA complex but reduces the affinity of the dye for dsDNA, (compare DC-21 and SH-0367 to the parent dye, Cyan-2). Increase of the polymethine chain length not only reduces the steric hindrance but also increases the affinity of a dye for dsDNA, (compare the K_d for DMB-2OH and DC-21 in water, Table 3). The higher affinity of DM for dsDNA relative to DM-1 is ascribed to the steric hindrance of the additional aromatic ring in DM-1. YO-PRO-1 exhibits a slightly higher affinity relative to DM-1 in ACES and TrisOAc, although the buffer average is similar (Table 3). This may be due to the

presence of cationic charges on the structure which are expected to improve the binding affinity due to the increased electrostatic attraction between dyes and the DNA phosphates [45].

The binding of the cyanine to dsDNA can be described by a model, which postulates that one or two of the dye heterocycles intercalates between the stacked bases in the double helix; while the remaining one accommodates into the helical grooves. Further, electrostatic interaction with phosphate groups of dsDNA stabilize binding [46, 47]. As magnesium ions bind preferentially to phosphate groups, the stability of dye–dsDNA complexes can be negatively affected by the concentration of Mg^{2+} [48]. Higher concentrations of Mg^{2+} would release more dye molecules from dsDNA into the solution, reducing the intensity of the dye–DNA complex and significantly increasing the background for single DNA molecule imaging (data not shown). To compare the ability of dye–DNA complexes to resist displacement by Mg^{2+}, the magnesium titration midpoint (MTMP) was used (Fig. 2 and Table 4). Cyan-2 and DM-1 have a higher MTMP, comparable to that of YO-PRO-1 (Table 4). In contrast, the MTMP for the remaining dyes, DC-21, DM, DMB-2OH, SH-0367 and SH1015-OH is 2–4 mM. Consequently, Cyan-2 and DM-1 were selected as the potential reporter molecules for DNA helicase activity.

Minor groove binding dyes bind preferentially to dsDNA but exhibit sequence-dependent binding [49–51]. In contrast, intercalating cyanine dyes are not only DNA sequence-independent but also exhibit a greater fluorescence enhancement on binding to DNA [52, 53]. However, those dyes can inhibit the activity of proteins involved in replication, repair and transcription [54–57]. A continuous fluorescence dye displacement DNA helicase assay was used to evaluate the potential inhibition of the novel dyes used in this study. The unwinding rate of RecBCD is largely unaffected by Cyan-2 and DM-1 relative to the control reactions carried out in the absence of dye, demonstrating that these two dyes do not inhibit RecBCD at the concentration of dyes tested, (i.e., 500 nM, producing an average DNA/dye ratio of 10: 1 (μM bp: μM dye)). Similarly, YO-PRO-1 does not significantly affect the rate of unwinding by RecBCD. Since Cyan-2 exhibits higher affinity to dsDNA and less affinity to ssDNA than YO-PRO-1 and DM-1, Cyan-2 is a better reporter molecule than YO-PRO-1 and DM-1 to precisely report the unwinding rate of RecBCD. In contrast, at the same dye concentration, YOYO-1 inhibits the helicase activity of RecBCD 6-fold relative to the reaction in the absence of dye and in the presence of the monomeric dyes. As YO-PRO-1 and YOYO-1 are similar in structure, the inhibition observed with YOYO-1 may be due to the dimeric version of this dye binding to the DNA with higher affinity, thereby impeding the progress of the enzyme.

The remaining cyanine dyes were also tested in the DNA helicase assay. Unexpectedly, these dyes do not follow the SSB unwinding trace. For DM, DMB-2OH and SH-0367, the fluorescence signal was too low to see any change during the reaction. As for DC-21 and SH1015-OH, the visible fluorescence signal was observed but no real change occurred during the reaction. These phenomena are probably due to the poor displacement of dyes from dsDNA or dyes rebinding subsequently to remaining dsDNA and ssDNA, even though SSB does bind to ssDNA under the condition used in the assay.

In summary, the data presented demonstrated that changes in the dye structure lead to significant changes in fluorescence intensity of dye–dsDNA complexes and the affinity of dyes for DNA. The fluorescence of a dye–DNA complex is affected in a complex manner by buffer type, pH and the presence of magnesium ions. From the group of seven novel dyes, Cyan-2 and DM-1 are excellent candidate molecules for further structural modification and for the construction of the dimeric forms of either Cyan-2, DM-1 or variants thereof.

References

1. Bustamante C, Bryant Z, Smith SB (2003) Ten years of tension: single-molecule DNA mechanics. Nature 421:423–427
2. Morikawa K, Yanagida M (1981) Visualization of individual DNA molecules in solution by light microscopy: DAPI staining method. J Biochem 89:693–696
3. Matsumoto S, Morikawa K, Yanagida M (1981) Light microscopic structure of DNA in solution studied by the 4′,6-diamidino-2-phenylindole staining method. J Mol Biol 152:501–516
4. Brewer L, Corzett M, Balhorn R (2002) Condensation of DNA by spermatid basic nuclear proteins. J Biol Chem 277:38895–38900
5. Brewer LR, Corzett M, Balhorn R (1999) Protamine-induced condensation and decondensation of the same DNA molecule. Science 286:120–123
6. Krishnamoorthy G, Roques B, Darlix JL, Mely Y (2003) DNA condensation by the nucleocapsid protein of HIV-1: a mechanism ensuring DNA protection. Nucleic Acids Res 31:5425–5432
7. Ladoux B, Quivy JP, Doyle P, du Roure O, Almouzni G, Viovy JL (2000) Fast kinetics of chromatin assembly revealed by single-molecule videomicroscopy and scanning force microscopy. Proc Natl Acad Sci U S A 97:14251–14256
8. Meng X, Cai W, Schwartz DC (1996) Inhibition of restriction endonuclease activity by DNA binding fluorochromes. J Biomol Struct Dyn 13:945–951
9. Matsuura S, Komatsu J, Hirano K, Yasuda H, Takashima K, Katsura S, Mizuno A (2001) Real-time observation of a single DNA digestion by lambda exonuclease under a fluorescence microscope field. Nucleic Acids Res 29:E79
10. Bennink ML, Scharer OD, Kanaar R, Sakata-Sogawa K, Schins JM, Kanger JS, de Grooth BG, Greve J (1999) Single-molecule manipulation of double-stranded DNA using optical tweezers: interaction studies of DNA with RecA and YOYO-1. Cytometry 36:200–208
11. Zaitsev EN, Kowalczykowski SC (1998) Binding of double-stranded DNA by Escherichia coli RecA protein monitored by a fluorescent dye displacement assay. Nucleic Acids Res 26:650–654

12. Perkins TT, Smith DE, Chu S (1997) Single polymer dynamics in an elongational flow. Science 276:2016–2021
13. Smith DE, Babcock HP, Chu S (1999) Single-polymer dynamics in steady shear flow. Science 283:1724–1727
14. Bianco PR, Brewer LR, Corzett M, Balhorn R, Yeh Y, Kowalczykowski SC, Baskin RJ (2001) Processive translocation and DNA unwinding by individual RecBCD enzyme molecules. Nature 409:374–378
15. Eggleston AK, Rahim NA, Kowalczykowski SC (1996) A helicase assay based on the displacement of fluorescent, nucleic acid-binding ligands. Nucleic Acids Res 24:1179–1186
16. Taylor AF, Smith GR (2003) RecBCD enzyme is a DNA helicase with fast and slow motors of opposite polarity. Nature 423:889–893
17. Haugland RP (2005) A guide to fluorescent probes and labeling technologies, 10th edn. Molecular Probes, Eugene, Oregon
18. Ernst LA, Gupta RK, Mujumdar RB, Waggoner AS (1989) Cyanine dye labeling reagents for sulfhydryl groups. Cytometry 10:3–10
19. Southwick PL, Ernst LA, Tauriello EW, Parker SR, Mujumdar RB, Mujumdar SR, Clever HA, Waggoner AS (1990) Cyanine dye labeling reagents—carboxymethylindocyanine succinimidyl esters. Cytometry 11:418–430
20. Mujumdar RB, Ernst LA, Mujumdar SR, Waggoner AS (1989) Cyanine dye labeling reagents containing isothiocyanate groups. Cytometry 10:11–19
21. Yarmoluk SM, Kovalska VB, Kovtun YP (1999) Interaction of cyanine dyes with nucleic acids. 5. Towards model of "half intercalation" of monomethyne cyanine dyes into double-stranded nucleic acids. Biopolymers and Cell (in Ukrainian) 15:75–82
22. Jason Wong C, Lucius AL, Lohman TM (2005) Energetics of DNA end binding by E.coli RecBC and RecBCD helicases indicate loop formation in the 3′-single-stranded DNA tail. J Mol Biol 352:765–782
23. Rhoades E, Gussakovsky E, Haran G (2003) Watching proteins fold one molecule at a time. Proc Natl Acad Sci U S A 100:3197–3202
24. Bengtsson M, Karlsson HJ, Westman G, Kubista M (2003) A new minor groove binding asymmetric cyanine reporter dye for real-time PCR. Nucleic Acids Res 31:e45
25. Glazer AN (1992) Stable dye–DNA intercalation complexes as reagents for high-sensitivity fluorescence detection. Nature 359:859–861
26. Rye HS, Yue S, Wemmer DE, Quesada MA, Haugland RP, Mathies RA, Glazer AN (1992) Stable fluorescent complexes of double-stranded DNA with bis-intercalating asymmetric cyanine dyes: properties and applications. Nucleic Acids Res 20:2803–2812
27. Kowalczykowski SC, Dixon DA, Eggleston AK, Lauder SD, Rehrauer WM (1994) Biochemistry of homologous recombination in *Escherichia coli*. Microbiol Rev 58:401–465
28. Akerman B, Tuite E (1996) Single- and double-strand photocleavage of DNA by YO, YOYO and TOTO. Nucleic Acids Res 24:1080–1090
29. Harmon FG, Kowalczykowski SC (2001) Biochemical characterization of the DNA helicase activity of the *Escherichia coli* RecQ helicase. J Biol Chem 276:232–243
30. Birnboim HC, Doly J (1979) A rapid alkaline extraction procedure for screening recombinant plasmid DNA. Nucleic Acids Res 7:1513–1523
31. Sambrook J, Fritsch EF, Maniatis T (1989) Molecular cloning: a laboratory manual, 2nd edn. Cold Spring Harbor Laboratory Press, Cold Spring Harbor, New York
32. Vinograd J, Lebowitz J (1966) Physical and topological properties of circular DNA. J Gen Physiol 49:103–125
33. Neuendorf SK, Cox MM (1986) Exchange of recA protein between adjacent recA protein–single-stranded DNA complexes. J Biol Chem 261:8276–8282
34. Lohman TM, Green JM, Beyer RS (1986) Large-scale overproduction and rapid purification of the *Escherichia coli ssb* gene product. Expression of the *ssb* gene under lambda PL control. Biochemistry 25:21–25
35. Lohman TM, Overman LB (1985) Two binding modes in Escherichia coli single strand binding protein–single stranded DNA complexes. Modulation by NaCl concentration. J Biol Chem 260:3594–3603
36. Handa N, Bianco PR, Baskin RJ, Kowalczykowski SC (2005) Direct visualization of RecBCD movement reveals cotranslocation of the RecD motor after chi recognition. Mol Cell 17:745–750
37. Roman LJ, Kowalczykowski SC (1989) Characterization of the helicase activity of the *Escherichia coli* RecBCD enzyme using a novel helicase assay. Biochemistry 28:2863–2873
38. Wolfbeis OS, Kostenko OM, Tolmachev OI, Yarmoluk SM (2001) US Patent no. 2003175988 DE 10153818A1
39. Hamers-Casterman C, Lagnaux M, Hamers R (1964) Sur la signification possible de l'absence d'un des allotypes dans les anticorps. Arch Int Physiol Biochim 72:685–686
40. Liu YY, Wang PY, Dou SX, Wang WC, Xie P, Yin HW, Zhang XD, Xi XG (2004) Ionic effect on combing of single DNA molecules and observation of their force-induced melting by fluorescence microscopy. J Chem Phys 121:4302–4309
41. Harmon FG, Kowalczykowski SC (2000) Coupling of DNA helicase function to DNA strand exchange activity. Methods Mol Biol 152:75–89
42. Matson SW, Kaiser-Rogers KA (1990) DNA helicases. Ann Rev Biochem 59:289–329
43. Gurrieri S, Wells KS, Johnson ID, Bustamante C (1997) Direct visualization of individual DNA molecules by fluorescence microscopy: characterization of the factors affecting signal/background and optimization of imaging conditions using YOYO. Anal Biochem 249:44–53
44. Yarmoluk SM, Kovalska VB, Kryvorotenko DV, Balanda AO, Ogul'chansky T (2001) Interaction of cyanine dyes with nucleic acids. XXV. Influence of affinity-modifying groups in the structure of benzothiazol-4-[2,6-dimethylpyridinium] dyes on the spectral properties of the dyes in the presence of nucleic acids. Spectrochim Acta, Part A: Mol Biomol Spectrosc 57:1533–1540
45. Manning GS (1978) The molecular theory of polyelectrolyte solutions with applications to the electrostatic properties of polynucleotides. Q Rev Biophys 11:179–246
46. Yarmoluk SM, Lukashov SS, Losytskyy MY, Akerman B, Kornyushyna OS (2002) Interaction of cyanine dyes with nucleic acids: XXVI. Intercalation of the trimethine cyanine dye cyan 2 into double-stranded DNA: study by spectral luminescence methods. Spectrochim Acta Part A Mol Biomol Spectrosc 58:3223–3232
47. Yarmoluk SM, Lukashov SS, Ogul'Chansky TY, Losytskyy MY, Kornyushyna OS (2001) Interaction of cyanine dyes with nucleic acids. XXI. Arguments for half-intercalation model of interaction. Biopolymers 62:219–227
48. Izatt RM, Christensen JJ, Rytting JH (1971) Sites and thermodynamic quantities associated with proton and metal ion interaction with ribonucleic acid, deoxyribonucleic acid, and their constituent bases, nucleosides, and nucleotides. Chem Rev 71:439–481
49. Cosa G, Focsaneanu KS, McLean JR, McNamee JP, Scaiano JC (2001) Photophysical properties of fluorescent DNA-dyes bound to single- and double-stranded DNA in aqueous buffered solution. Photochem Photobiol 73:585–599
50. Moon JH, Kim SK, Sehlstedt U, Rodger A, Norden B (1996) DNA structural features responsible for sequence-dependent binding geometries of Hoechst 33258. Biopolymers 38:593–606
51. Kubista M, Akerman B, Norden B (1987) Characterization of interaction between DNA and 4′,6-diamidino-2-phenylindole by optical spectroscopy. Biochemistry 26:4545–4553
52. Nygren J, Svanvik N, Kubista M (1998) The interactions between the fluorescent dye thiazole orange and DNA. Biopolymers 46:39–51

53. Rye HS, Glazer AN (1995) Interaction of dimeric intercalating dyes with single-stranded DNA. Nucleic Acids Res 23:1215–1222
54. Jeggo PA (1998) Identification of genes involved in repair of DNA double-strand breaks in mammalian cells. Radiat Res 150:S80–S91
55. Jeggo PA, Tesmer J, Chen DJ (1991) Genetic analysis of ionising radiation sensitive mutants of cultured mammalian cell lines. Mutat Res 254:125–133
56. Lees-Miller SP, Godbout R, Chan DW, Weinfeld M, Day RS 3rd, Barron GM, Allalunis-Turner J (1995) Absence of p350 subunit of DNA-activated protein kinase from a radiosensitive human cell line. Science 267:1183–1185
57. George JW, Ghate S, Matson SW, Besterman JM (1992) Inhibition of DNA helicase II unwinding and ATPase activities by DNA-interacting ligands. Kinetics and specificity. J Biol Chem 267:10683–10689